

Supporting Information

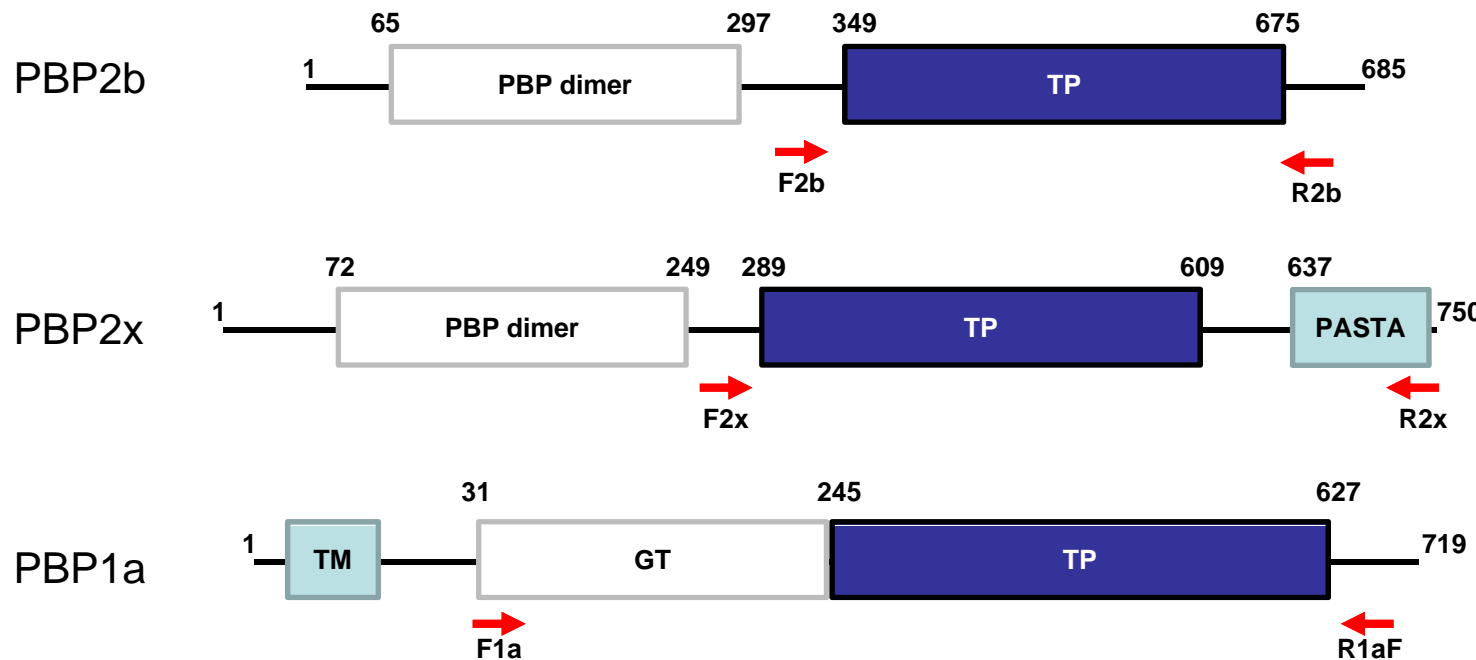


Fig. S1. Graphical representation of the *pbp* genes showing the different amplified regions used to transform the Cp1015 strain to obtain single, double and triple *pbp* mutants. The arrows represent the position of the primers used to amplify each *pbp* region.

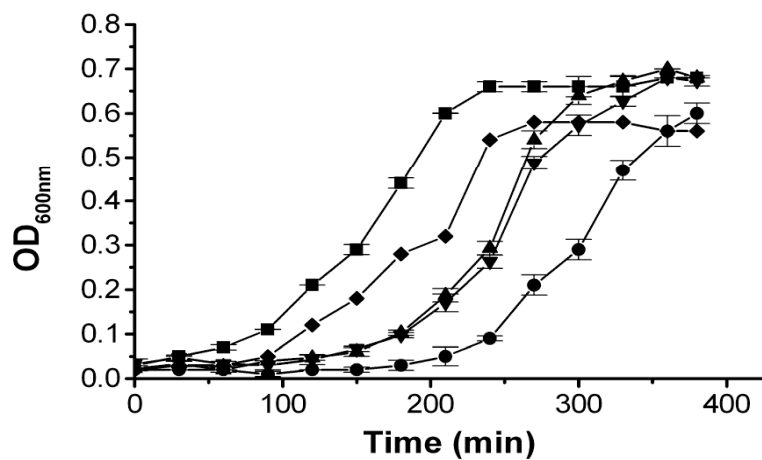


Fig. S2. Effect of *pbp* mutations on growth curves. Growth curves of *S. pneumoniae* were incubated in Todd Hewitt broth supplemented with 0.01% albumin at 37°C for CP1015 wt (■), CP1015 *pbp2b*²⁸ (●), CP1015 *pbp2b*²⁸ *pbp1a*²⁸ (▽), CP1015 *pbp2b*²⁸ *pbp2x*²⁸ (▲), and CP1015 *pbp2b*²⁸ *pbp2x*²⁸ *pbp1a*²⁸ (♦).

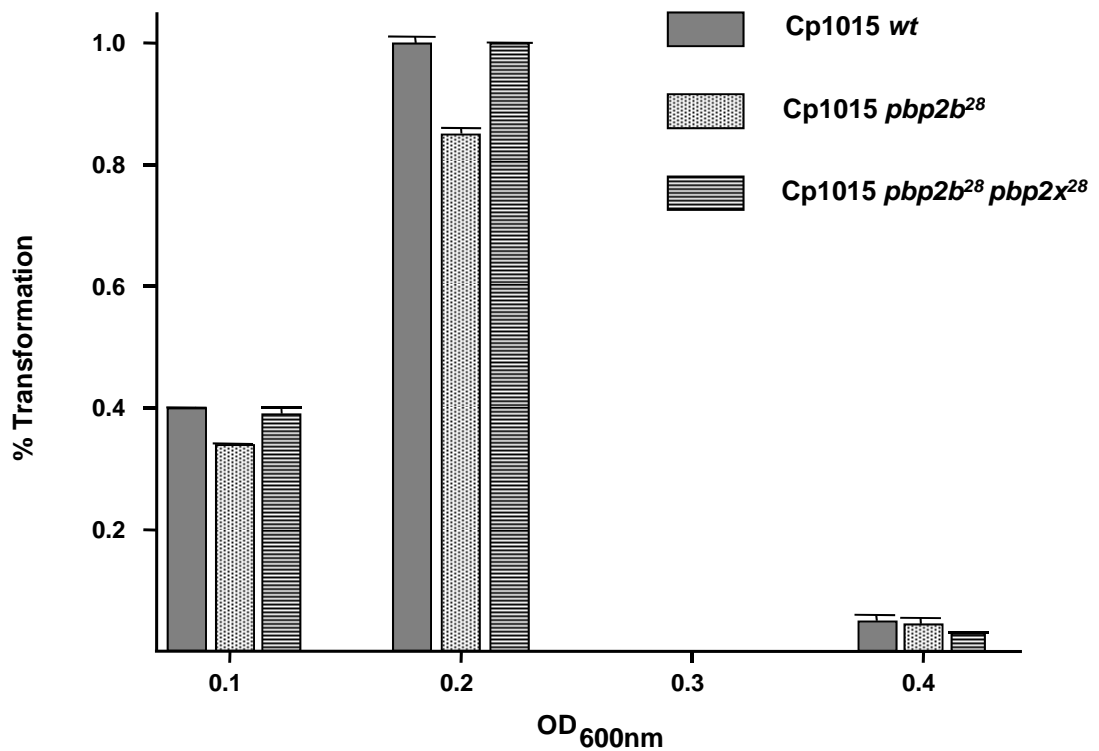


Fig. S3. Natural competence assay. *S. pneumoniae* Cp1015 *wt*, *pbp2b*, and *pbp2b pbp2x* mutants were grown in CTM medium. The percentage of transformation (ratio of cfu on rifampicin agar plates and cfu on agar plates without antibiotic) indicates the bacterial capacity of DNA incorporation and recombination. The *pbp* mutants showed the typical maximum transformation level at OD_{600nm} 0.1-0.2 as found for the Cp1015 *wt* strain.

Fig. S4. Amino acid substitutions found in PBP2b proteins obtained from different clinical strains. The sequences shown correspond to the TP region from Cp1015 (WT), Spain^{9V}-3 clone (Sp) and the clinical strains 12, 19, 28, 52, 56 and 62. The Cp1015 sequence is shown as a reference; identical sites are represented by dots, with only polymorphisms being indicated. The amino acid position are indicated vertically. Amino acids in bold represent common substitutions.

Fig. S5. Amino acid substitutions found in PBP2x proteins obtained from different clinical strains. The sequences shown were obtained from Cp1015 (WT), Spain^{9V}-3 clone (Sp) and the clinical strains Cba-12, Cba-52, Cba-56 and Cba-62. Identical sites **in other strains** are represented by dots, with only polymorphisms being indicated. The amino acid position of the polymorphic sites is indicated vertically. The N278 substitution is shown in bold.

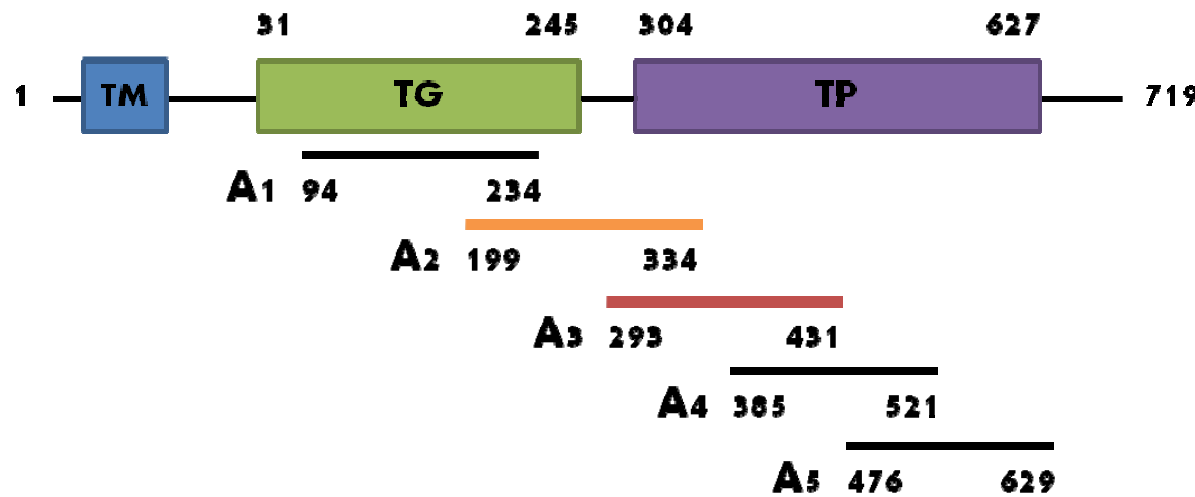


Fig. S6. Graphical representation of the *pbp1a* gene showing the different regions used to transform the Cp1015 *pbp2b²⁸* mutant to obtain the Cp1015 *pbp2b²⁸ pbp1a²⁸*-A2 and Cp1015 *pbp2b²⁸ pbp1a²⁸*-A3 mutants. A2 and A3 sequence analysis allowed the evaluation of the contribution of amino acidic substitutions in cefotaxime resistance and *fitness* compensation.

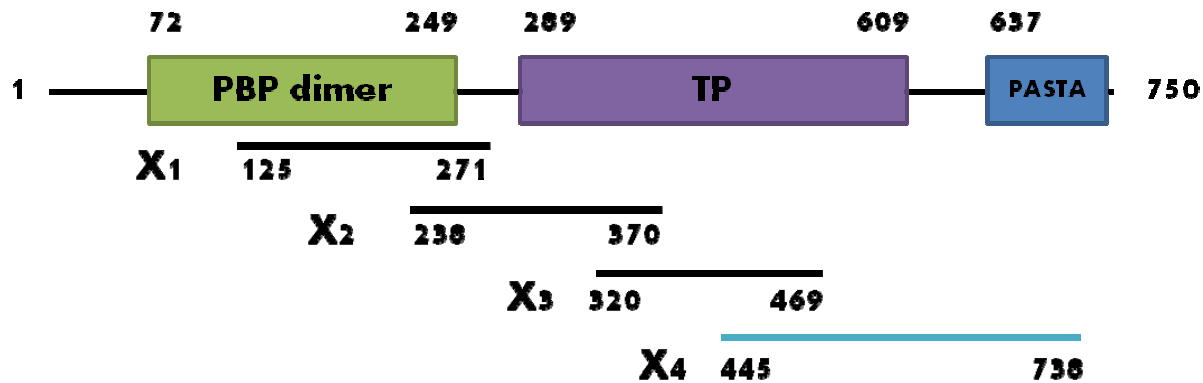


Fig. S7. Graphical representation of the *pbp2x* gene showing the region used to transform the Cp1015 *pbp2b²⁸* mutant to obtain the Cp1015 *pbp2b²⁸pbp2x²⁸*-X4mutant. The X4 sequence analysis allowed the evaluation of the contribution of amino acidic substitutions in cefotaxime resistance and *fitness* compensation.

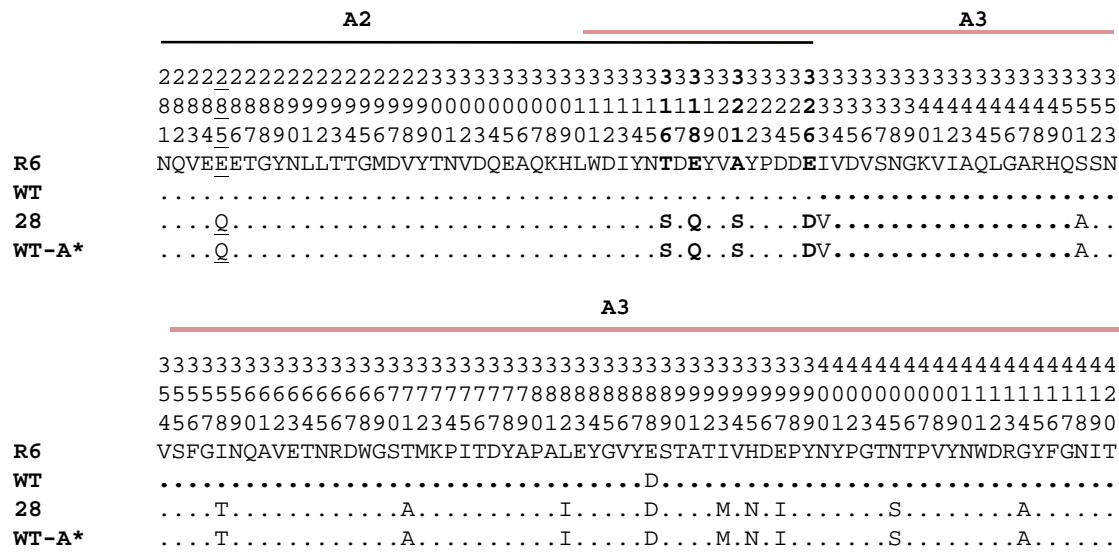


Fig. S8. Amino acid substitutions found in the transpeptidase region of PBP1a in the *pbp2b²⁸ pbp1a²⁸* mutant. The amino acid sequences shown correspond to the A2 and A3 regions from Cp1015 (WT), strain Cba-28 (28) and the Cp1015 *pbp2b²⁸* A2/A3*pbp1a²⁸* mutant (WT-A*). The R6 sequence is shown as a reference; identical sites in other strains are represented by dots, with only the polymorphisms being indicated. The amino acid position of the polymorphic sites is indicated vertically. Amino acids in bold are the substitutions involved in resistance, and the underlined residue is probably related to fitness compensation.

	33334444444444444444444444445555555555556
	9999122233344444455677888889246777778891
	1234778901734567890108901234541360123463772
	**** * ***
WT	SVVKNSWYTQQALEYSSN <u>T</u> L <u>S</u> A M <u>EKLR<u>S</u>TANDQLQPTMDSAG</u>
WT-2b ¹⁹PY....KLE..... <u>A</u> IT.....A.S.....
WT-2b ²⁸PY....KLE..... <u>A</u> IT.....A.S.....
Cba-19PY....KLE..... <u>A</u> IT.. <u>G</u> ...AAS.....
Cba-28PY....KLE..... <u>A</u> IT.. <u>G</u> ...AAS.....
607TPY....KLE..... <u>A</u> IT.. <u>G</u> ...AA.DEAIDTKIEAS.
608PY....KLE..... <u>A</u> IT.. <u>G</u> ...AA.DEAIDTKIEAS.
901TPY....KLE..... <u>A</u> IT.. <u>G</u> ...AA.....
902PY....KLE..... <u>A</u> IT.. <u>G</u> ...AAS.....

Fig. S9. Comparison of amino acid sequences of PBP2b mutants. The sequences shown correspond to the TP region from the Cp1015 (WT), Cba-19 and Cba-28 clinical strains, and the Cp1015 *pbp2b*¹⁹ (WT-2b²⁸) and Cp1015 *pbp2b*²⁸ (WT-2b²⁸) mutants. Identical sites in other strains are represented by dots, with only the polymorphisms being indicated. The amino acid position of the polymorphic sites are indicated vertically. Asterisks show the TP active sites. Amino acids in bold and underlined indicate the most common substitutions found in resistant isolates. Sequences are also compared to those described by Trzcinski *et al* (607T, 608, 901T and 908).

	222222223333333333333333333333333333333333333
	666666681133334444444555566666666
	123456781125678901234567856789012345678

WT	VYTTISSLQDAPGST <u>M</u> KVMLAAGIGEVFNSSELKIAD
WT-2x ¹⁹	ESS.....LN..... AT..SS.S..Y.....F....
WT-2x ²⁸	ESS.....LN..... AT..SS.S..Y.....F....
Cba-19	ESS.....LN..... AT..SS.S..Y.....F....
Cba-28	ESS.....LN..... AT..SS.S..Y.....F....
607TTLN..... AT..SSVS..Y.....F....
608TLN..... AT..SS.S..Y.....F....
901TL...LN..... AT..SS.S..Y.....F....
902L...LN..... AT..SS.S..Y.....F....
	333333333333333333333333333333334444444444444
	67777888888888999999999990014688889999
	90189012345678901234567890174267890123

WT	AT <u>I</u> EGLTGG <u>R</u> MMTFSQGFAHSSNVGMTNNIPNDQTARK
WT-2x ¹⁹	.. <u>T</u> D....T. <u>G</u>L.....SKL.....
WT-2x ²⁸	.. <u>T</u> D....T. <u>G</u>L.....SKL.....
Cba-19	.. <u>T</u> D....T. <u>G</u>L.....SKL.....
Cba-28	.. <u>T</u> D....T. <u>G</u>L.....SKL.....
607T	.. <u>T</u> D....T. <u>G</u>L.....SKSLT.N.SV..
608	.. <u>T</u> D....T. <u>G</u>L.....SKSLT.N.SV..
901T	.. <u>T</u> D....T. <u>G</u>L.....SKSLT.N.SV..
902	.. <u>T</u> D....T. <u>G</u>L.....SKSLT.N.SV..

Fig. S10. Comparison of amino acid sequences of PBP2x mutants. The sequences shown correspond to the TP region from the Cp1015 (WT) Cba-19 and Cba-28 clinical strains, and the Cp1015 *pbp2b*¹⁹ (WT-2x¹⁹), and Cp1015 *pbp2b*²⁸ (WT-2x²⁸) mutants. Identical sites in other strains are represented by dots, with only the polymorphisms being indicated. The amino acid position of the polymorphic sites are indicated vertically. Asterisks show the TP active sites. Amino acids in bold and underlined indicate the most common substitutions found in resistant isolates. Sequences are also compared to those described by Trzcinski et al (607T, 608, 901T and 902).

Fig. S11. Comparison of amino acid sequences of PBP1a mutants. The sequences shown correspond to the TP region from the Cp1015 (WT), Cba-19 and Cba-28 clinical strains, and the Cp1015 *pbp2b*¹⁹ (WT-1a¹⁹), Cp1015 *pbp2b*²⁸ (WT-1a²⁸) mutants. The R6 sequence is shown as a reference, and identical sites in other strains are represented by dots, with only polymorphisms being indicated. The amino acid position of the polymorphic sites are indicated vertically. Asterisks show the TP active sites. Amino acids in bold and underlined indicate the most common substitutions found in resistant isolates. Sequences are also compared to those described by Trzcinski *et al* (607T, 608, 901T and 908).

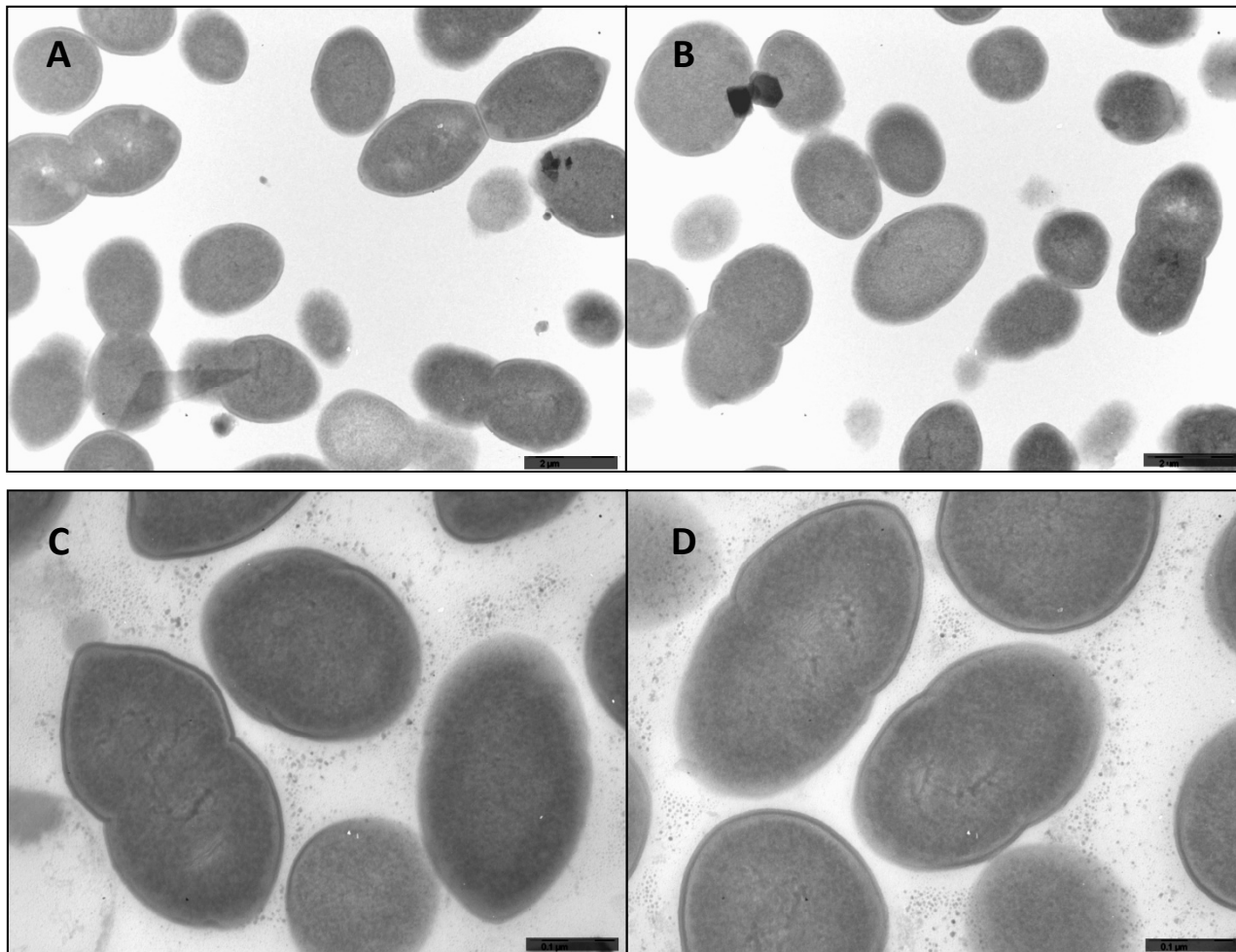


Fig. S12. Electron microscopy analysis of cellular morphology of strain Cp1015 (wt) Microphotographs of four different fields revealed the typical morphology of *S. pneumoniae*, with correct septum placement, division and symmetry of daughter cells. This data is complementary to that shown in Fig. 2 (A and B, bar scale 1.6 μm ; C and D, bar scale 0.8 μm).

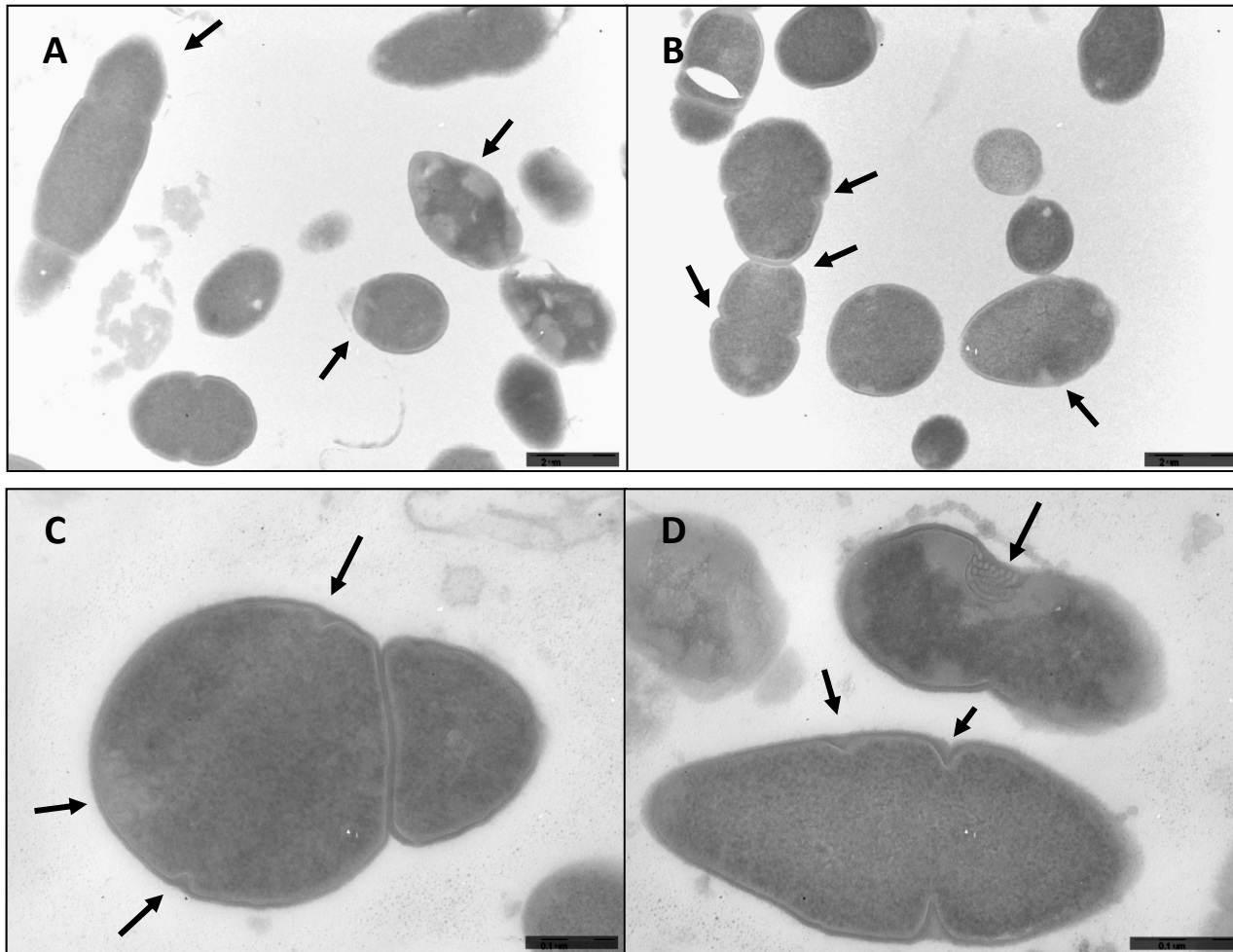


Fig. S13. Electron microscopy analysis of the effect of *ppb2b* mutations on cellular morphology. Microphotographs of different fields obtained for the *ppb2b* mutant. Arrows indicate multiple septa and irregularities, consistent with the accumulation of the cell wall, and atypical septum localization resulting in irregular cell divisions and asymmetrical daughter cells. This data is complementary to that shown in Fig. 2. (A and B, bar scale 1.6 μm ; C and D, bar scale 0.8 μm).

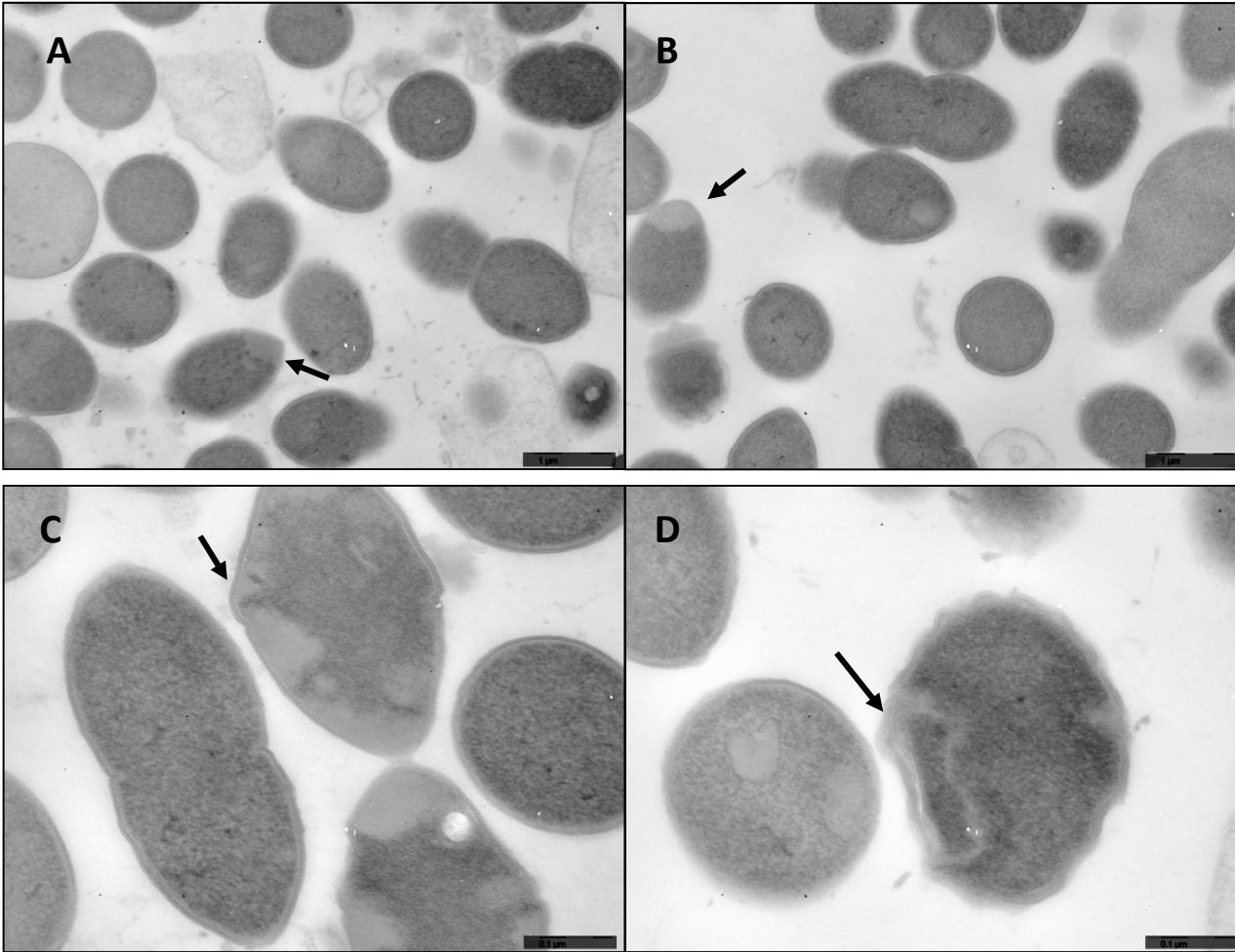


Fig. S14. Electron microscopy analysis of the effect of *pfp2b* *pfp2X* mutations on cellular morphology. Microphotographs of different fields obtained for the *pfp2b* *pfp2x* mutant. Arrows indicate irregularities consistent with the accumulation of the cell wall and atypical septum localization. This data is complementary to that shown in Fig. 2. (A and B, bar scale 1.6 μm ; C and D, bar scale 0.8 μm).

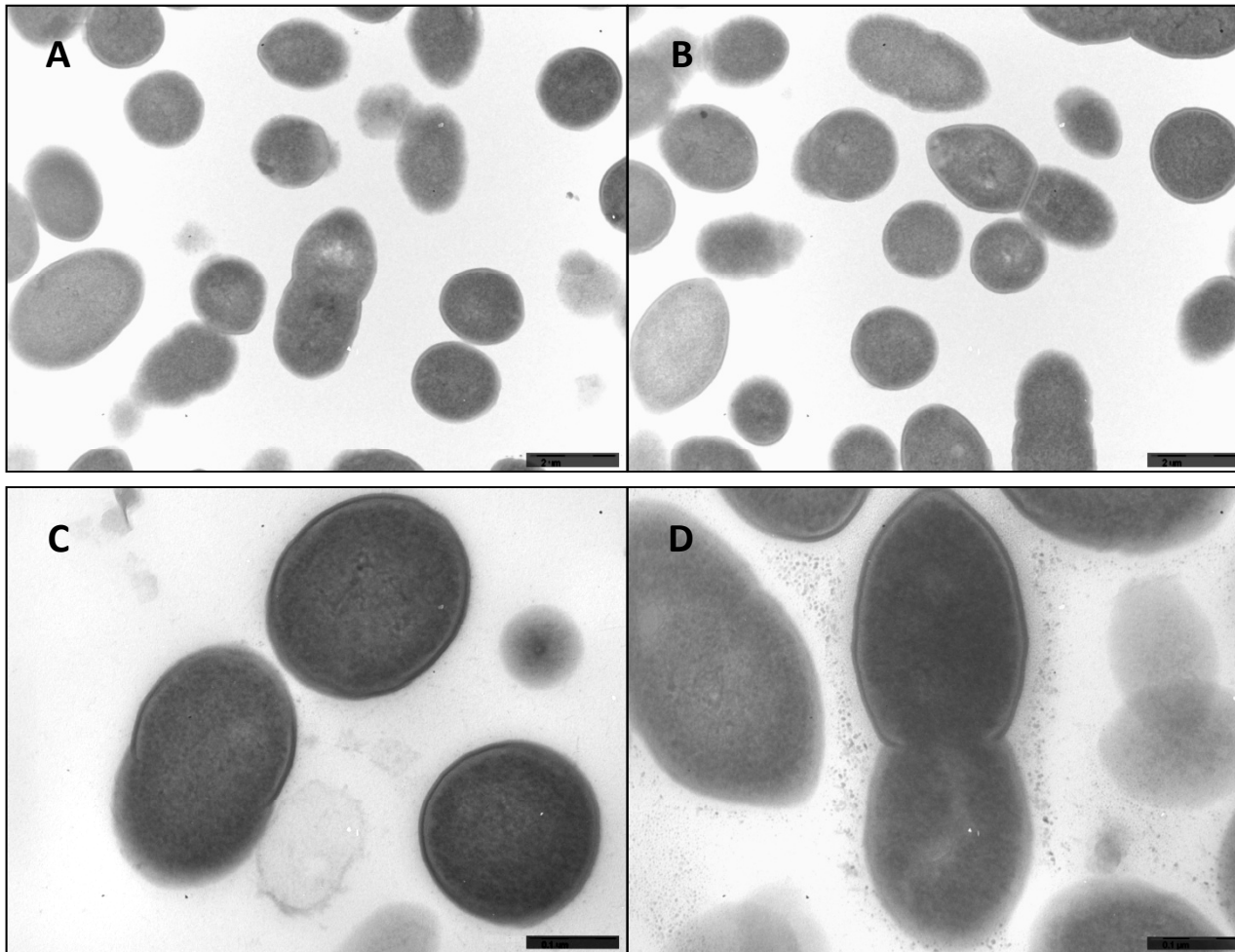


Fig. S15. Electron microscopy analysis of the effect of *pbp2b pbp2x pbp1a* mutations on cellular morphology. Microphotographs of different fields revealed no apparent abnormalities for the *pbp2b pbp2x pbp1a* mutant, which showed a similar morphology to that of wild-type cells. This data is complementary to that shown in Fig. 2. (A and B, bar scale 1.6 μm ; C and D, bar scale 0.8 μm).

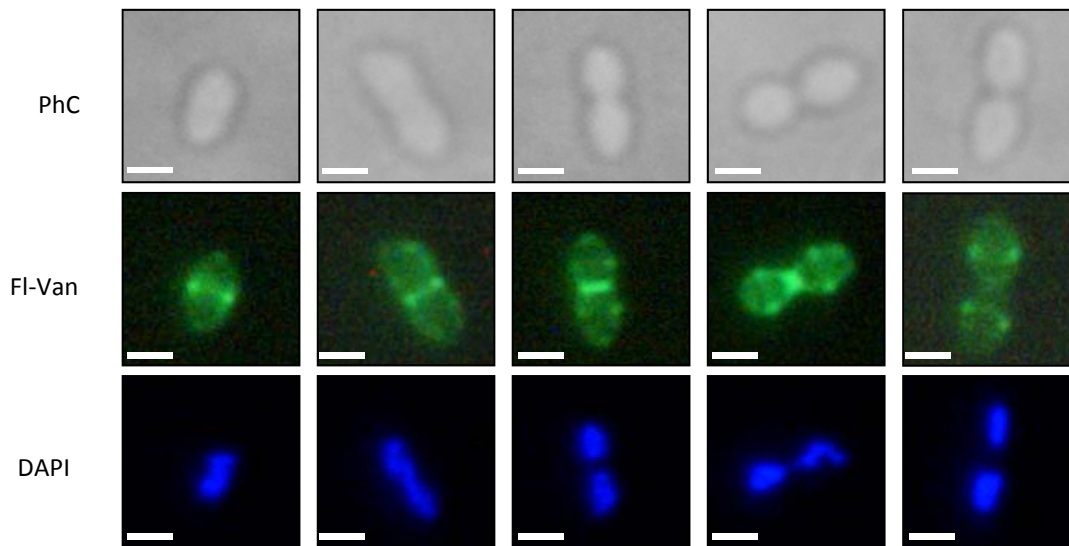


Fig. S16. Peptidoglycan synthesis of strain Cp1015 (*wt*) at different stages in the cell cycle. Cp1015 was grown exponentially in Todd Hewitt broth at 37°C. Cells were stained with fluorescent vancomycin (Fl-Van) and DAPI, and viewed by using an epifluorescent microscope (see *Material and Methods*). Images were assigned to stages of the cell cycle on the basis of the extent of nucleoid segregation, cell elongation and septum constriction. Multiple fields were examined for numerous independent experiments, with representative images being shown (bar scale, 1 μm).

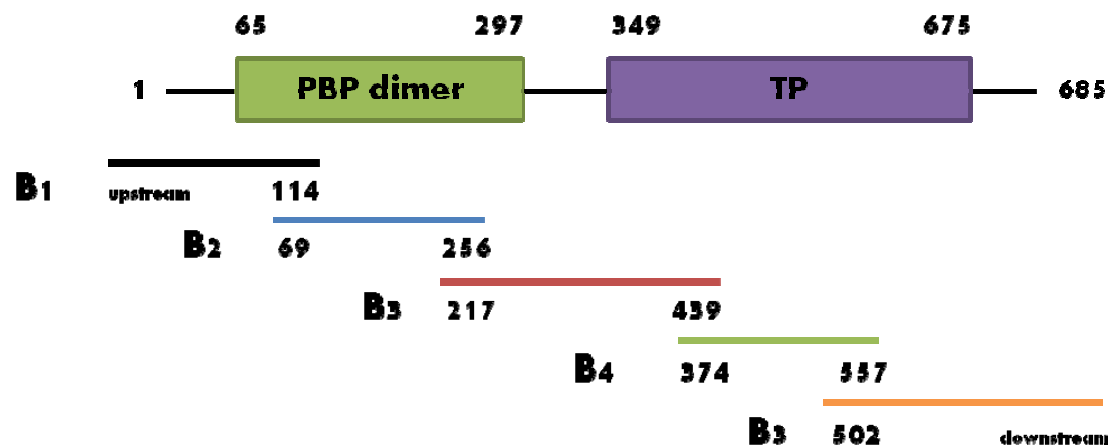


Fig. 17. Graphical representation of the *pbp2b* gene showing the different DNA fragments, amplified by PCR from clinical strains and sequenced (See Materials and Methods).